High-Density, Low Temperature Ignited Operations in FFHR

Osamu MITARAI, Akio SAGARA[1)], Ryuichi SAKAMOTO[1)], Nobuyoshi OHYABU[1)], Akio KOMORI[1)] and Osamu MOTOJIMA[1)]

Liberal Arts Education Center, Kumamoto Campus, Tokai University, 9-1-1 Toroku, Kumamoto 862-8652, Japan
[1)]*National Institute for Fusion Science, 322-6 Oroshi-cho, Toki, 509-5292, Japan*

(Received 6 January 2009 / Accepted 8 June 2009)

New control method of the unstable operating point in the helical reactor FFHR makes the ignition study on the high density and low temperature operation possible. Proportional-integral-derivative (PID) control of the fueling with the error of the fusion power of $e'_{\rm DT}(P_{\rm f}) = -(P_{\rm fo} - P_{\rm f})$ can stabilize the unstable operating point. Here $P_{\rm fo}(t)$ is the fusion power preset value and $P_{\rm f}(t)$ is the measured fusion power. Although the large parameter variation would lose its control due to the inherently unstable nature, it is possible to control the ignited operation by pellet injection with the pellet size between 12 mm and 16 mm. Unstable ignited operation is robust against disturbances such as impurity increments by fueling feedback alone. However, if the heating power feedback control is added, robustness to the disturbances is improved, and an operational regime with respect to the integration time and derivative time is expanded.

Keywords: helical reactor, thermally unstable, high density, low temperature, ignition

DOI: 10.1585/pfr.5.S1001

1. Introduction

Achievement of the superdense-core (SDC) plasmas in LHD experiments [1, 2] stimulates the study on the stabilization method of the thermal instability in a fusion reactor. Recently, new, simple and comprehensive control method of the unstable operating point is proposed for the high-density and low temperature ignited operation for the FFHR helical reactor [3, 4]. PID feedback control of the fueling based on the error of the fusion power with an opposite sign of $e'_{\rm DT}(P_{\rm f}) = -(P_{\rm fo} - P_{\rm f})$ can stabilize the unstable operating point and the desired fusion power is obtained at the same time. Here $P_{\rm f}$ is the measured fusion power and $P_{\rm fo}$ is its preset value. Using this control algorithm, the operating point with the box type density profile can reach the high-density and low temperature steady state condition ($n(0) \sim 1 \times 10^{21}$ m^{-3}, $T(0) \sim 6.4$ keV, and $<\beta> \sim 2.5$ %) from the initial very low temperature and density regime [5]. Although this control was demonstrated using the zero-dimensional analysis, it can be also applied to one-dimensional simulation code and implemented in a reactor because linearization is not necessary in equations different from previous studies [6–11].

Although the high-density and low temperature ignited operation is inherently unstable, it is demonstrated that the steady state can be maintained even when plasma parameters are disturbed by pellet injections [5]. So far feedback control was used for fueling, and not for the external heating power [4, 5]. Although preprogramming of the heating power is enough for ignited operation in FFHR in many cases, it may expand the operational capability if it can be developed.

In this study we demonstrate that feedback control of the external heating power is possible and expands the operational regime for ignited operation. Especially, it improves control robustness to disturbances such as the change in the impurity fraction than that without the feedback control of the heating power.

2. Zero-Dimensional Equations and Density Profiles of SDC Plasma

In this analysis, the global power balance equation is used,

$$\frac{{\rm d}W}{{\rm d}t} = P_{\rm EXT} - (P_{\rm L} + P_{\rm B} + P_{\rm S} - P_{\alpha}) \qquad (1)$$

where $P_{\rm EXT}$ is the external heating power, $P_{\rm L}$ is the total plasma conduction loss, $P_{\rm B}$ is the total bremsstrahlung loss, $P_{\rm S}$ is the total synchrotron radiation loss, which is negligible in the low temperature operation, and P_{α} is the total alpha heating power. The ISS95 confinement scaling is used for the plasma conduction loss where $\gamma_{\rm ISS}$ represent the confinement enhancement factors over the ISS95 scaling [12]. The Plasma Operating Contour map (called as POPCON) is the contour map of the heating power of $P_{\rm HT} = (P_{\rm L} + P_{\rm B} + P_{\rm S} - P_{\alpha})$ plotted on the n-T plane. Sudo density limit scaling on the line density is used as a measure of core plasma density with the density limit factor of $\gamma_{\rm SUDO} = 5.5$ over the Sudo density limit [13]. In the power balance equation the equal ion and electron temperature was assumed due to very high density [3–5].

The combined particle balance equation using the

author's e-mail: omitarai@ktmail.tokai-u.jp

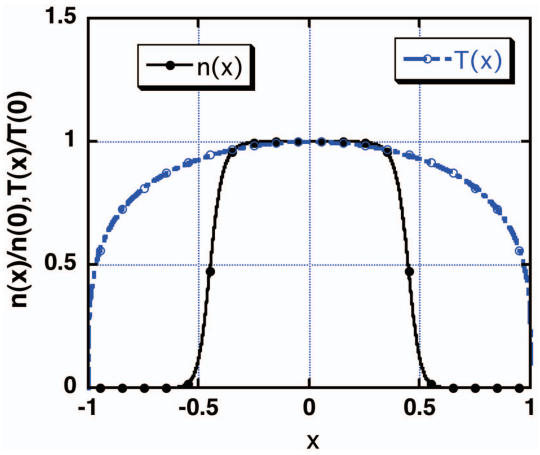

Fig. 1 Assumed box type SDC density and temperature profiles.

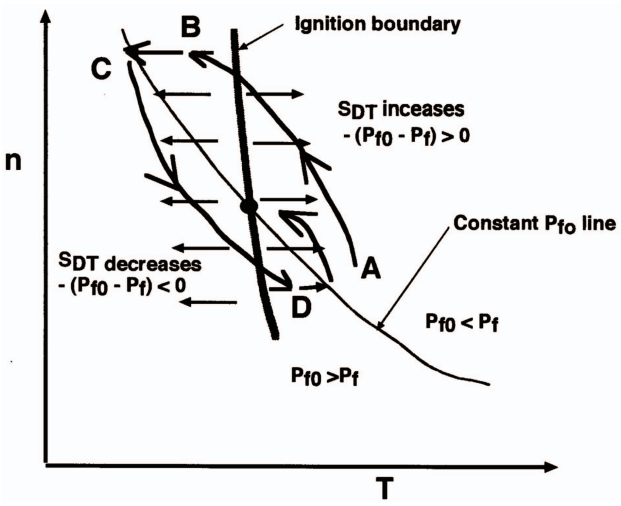

Fig. 2 Schematic movement of the operating point around the unstable ignition point on POPCON for continuous fueling [3–5].

charge neutrality condition is

$$\frac{dn_e(0)}{dt} = \frac{1}{1-8f_o}\left[(1+\alpha_n)S_{DT}(t) - \left\{\frac{f_D+f_T}{\tau_p^*}+\frac{2f_\alpha}{\tau_\alpha^*}\right\}n_e(0)\right] \quad (2)$$

where f_o is the oxygen impurity fraction, α_n is the density profile factor, S_{DT} is the D-T fueling rate, f_D is the deuterium fraction, f_T is the tritium fraction, f_α is the helium ash fraction, τ_p^* is the D-T fuel particle confinement time, and τ_α^* is the helium ash confinement time. The helium ash confinement time ratio of $\tau_\alpha^*/\tau_E = 3$, and the fuel particle confinement time ratio of $\tau_p^*/\tau_E = 3$ have been assumed in the helium ash particle balance equation unless otherwise noted. We assumed the box type density profile $n(x)$ for SDC plasma using hyperbolic tangent, and used the broad temperature profile $T(x)$ with $\alpha_T = 0.25$ [5] as shown in Fig. 1.

3. Unstable Ignition Control Algorithm

3.1 Feedback control of fueling

Stable ignition in FFHR reactor is controlled by the continuous D-T fueling rate:

$$S_{DT}(t) = S_{DT0}G_{fo}(t)\left\{e_{DT}(P_f) + \frac{1}{T_{int}}\int_0^t e_{DT}(P_f)dt + T_d\frac{de_{DT}(P_f)}{dt}\right\} \quad (3)$$

where the PID control is used based on the fusion power error of $e_{DT}(P_f) = +(1 - P_f(t)/P_{fo}(t))$, where $P_{fo}(t)$ is the fusion power preset value and $P_f(t)$ is the measured fusion power [13]. However, the opposite sign of $e_{DT}(P_f) = -(1 - P_f(t)/P_{fo}(t))$ can stabilize the thermal instability [3–5].

This behavior is understood as shown in POPCON in Fig. 2 for the continuous fueling. When P_f is larger than P_{fo}, the operating point (A) moves toward the higher density and lower temperature side. This operating point slightly shifts to the higher temperature side due to ignition nature between (A) and (B). When it enters in the sub-ignition regime (B), it goes to the lower temperature side due to sub-ignition nature and crosses the constant P_{fo} line (C). The fueling is now decreased and the operating point proceeds to the lower density and higher temperature side, and goes into the ignition regime (D), and crosses the constant P_{fo} line. Thus, oscillations take place and are damped away.

On the other hand, fueling is digitized for pellet injection. The PID signal *Error* (P_f), based on the fusion power error of $e_{DT}(P_f) = -(1 - P_f(t)/P_{fo}(t))$,

$$Error(P_f) = \left\{e_{DT}(P_f) + \frac{1}{T_{int}}\int_0^t e_{DT}(P_f)dt + T_d\frac{de_{DT}(P_f)}{dt}\right\} \quad (4)$$

determines the timing when the pellet is injected or not. Injected fueling quantity is discriminated by

$$\begin{cases} S_{DT}(t) = S_{DTpellet} & for\ \ Error(P_f) > 0 \\ S_{DT}(t) = 0 & for\ \ Error(P_f) \le 0 \end{cases} \quad (5)$$

where $S_{DTpellet}$ is the fueling particle number per the plasma volume by one pellet as given below. In this case the operation path moves straightly, and crosses the unstable ignition boundary along the constant beta line.

3.2 Pellet size

As the D-T solid molar volume is 19.88 mm^3/mol [14], D-T ice density is given by $6.02\times10^{23} \times 2/19.88$ [mm^3/mol] $= 6.05\times10^{28}$ m^{-3}. For the pellets with a diameter $D_p = 14$ mm and length $L_p = 14$ mm, the total D-T particle number is $N_{pell} = \pi(D_{pp}/2)^2L_p\times6.05\times10^{28} = 130\times10^{21}$. Therefore, fueling particle number per plasma volume of $V_o = 827$ m^3 is $S_{DTpell} = 1.57\times10^{20}$ m^{-3}/(1 pellet pulse) , which corresponds to fueling rate in the continuous fueling operation (see Fig. 3 (d)). Three pellets are

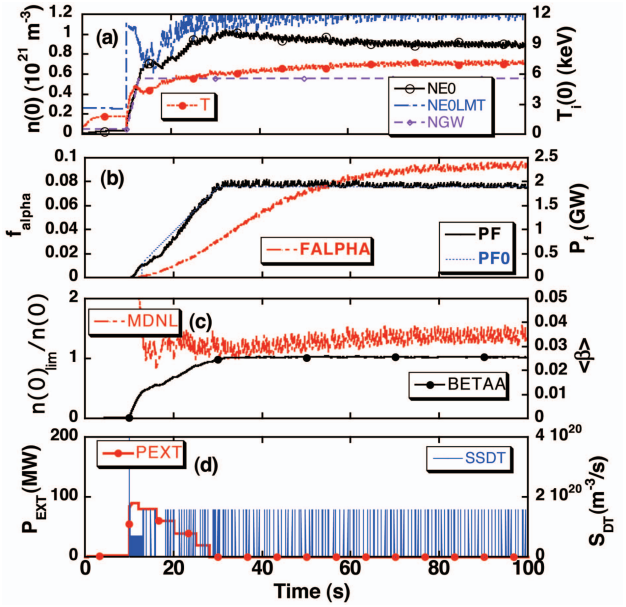

Fig. 3 Temporal evolution of the plasma parameters for τ_α^*/τ_E = 5 and the pellet size of 14 mm. (a) Peak temperature, peak density, density limit, (b) alpha ash fraction, fusion power and its set value, (c) density limit margin, beta value, and (d) D-T pellet fueling rate, and the heating power. (T_{int} = 8 s and T_d = 0.26 s). The density variation is $\Delta n \sim 5 \times 10^{19}$ m^{-3}.

injected consecutively with the time step of Δt = 0.02 s for better pellet penetration, and next three steps are prohibited for injection. We note that in the following figures three pellet injections are described by one rectangular box. Therefore, the overall repetition time of pellet injection seems to be 0.02 s × 6 = 0.12 s, where the calculation time step is Δt = 0.02 s. In this study this pellet injection scheme is taken as a reference. Detailed pellet injection algorithm was described in the reference [15]. If this overall pellet injection repetition time is reduced, the plasma parameter oscillation would be reduced, which needs more detailed study.

3.3 Feedback control of the heating power

In the stable ignition the external heating power is feedback controlled using the density limit scaling [16]. However, as it is difficult to use the density limit scaling in the unstable operation, the different control algorithm must be developed. In this study we used the fusion power error as used in the ITER ignition study [17]. When the fusion power is smaller than the preset value, the heating power is applied by the following algorithm.

$$P_{EXT}(P_f) = P_{EXTO}\left\{e_{EXT}(P_f) + \frac{1}{T_{Pint}}\int_0^t e_{EXT}(P_f)dt\right\} \quad (6)$$

where P_{EXT0} = 500 MW, $e_{EXT}(P_f) = (1 - P_f(t)/P_{fimp}(t))$, and P_{fimp} is the preset value given by $P_{fimp}(t) = P_{fo}(t)$ (1.8/1.9). In the steady state P_{fimp} = 1.8 GW is lower than 1.9 GW in order to prevent the heating power application during the fusion power oscillation. Here, PI feedback control has been used with T_{Pint} = 15 s.

4. Ignition Access to the Unstable Operating Point

Figure 3 shows the temporal evolution of plasma parameters for the pellet size of L_p = 14 mm in FFHR2 m with R = 14 m, $\bar{a}$ = 1.73 m, B_o = 6 T, P_f = 1.9 GW, γ_{ISS} = 1.6, and τ_α^*/τ_E = 5. For the fusion power rise-up time of $\Delta\tau_{rise}$ = 20 s and the maximum external heating power of P_{EXT} = 90 MW, the time averaged density is initially built up to $\sim 0.6 \times 10^{21}$ m^{-3} by the density feedback (NGW trace) until 12.8 s and then raised up to $n(0) \sim 1 \times 10^{21}$ m^{-3} and decreased to 8.9×10^{20} m^{-3} by the fusion power control switched on at 12.8 s. In more detail, between 10 s and 12.8 s, the density is controlled by the error of the density as given by

$$e_{DT}(n) = +(1 - n(t)/n_{GW}(t)) \quad (7)$$

where $n_{GW}(t)$ is the preset value of the density waveform with the linearly increasing function. At 12.8 s the density control is switched to the fusion power control as given by Eq. (3) with $e_{DT}(P_f) = -(1 - P_f(t)/P_{fo}(t))$ for thermally unstable operation. The detailed schematic waveform on this transition phase is shown in Fig. 4.

Between 10.0 s and 12.8 s as seen in Fig. 3 (d), the pellet fueling rate is smaller than that after 12.8 s. This is to study the overall behavior of the pellet injection effect on the unstable ignition regime. We fixed operation parameters between 10.0 s and 12.8 s because pellet injection needs careful adjustment and the control algorithm is not suited for the thermally unstable regime. Therefore, to use the same pellet size in the entire discharge duration, operation should be more optimized between 10 s and 12.8 s in the future.

The external heating power is preprogrammed to decrease it to 0 at 24 s. We see that even by fueling at the discrete time the ignition access is possible. When the density is increased by three consecutive pellets, the temperature is dropped. Their variations are out of phase due to adiabatic process by the power balance equilibrium in a short time. We found that the density variation of $\Delta n \sim 5 \times 10^{19}$ m^{-3} is allowed for ignited operation.

Especially for larger τ_α^*/τ_E = 5, the time averaged peak temperature at the steady state is $T_i(0) \sim 7.14$ keV, the volume averaged beta value is $<\beta> \sim 2.55$ %, the helium ash fraction is 8.9 %, the effective charge is $Z_{eff} \sim 1.60$, and the average neutron wall loading is $\Gamma_n \sim 1.5$ MW/m^2.

Alpha ash confinement time ratio τ_α^*/τ_E plays an important role in a high density operation. Together with the confinement factor, ignition regime is determined by the alpha ash confinement time ratio. Such dependence was studied in detail in the previous paper [5]. Wide parameter regime with τ_α^*/τ_E = 3~8 was surveyed to obtain ig-

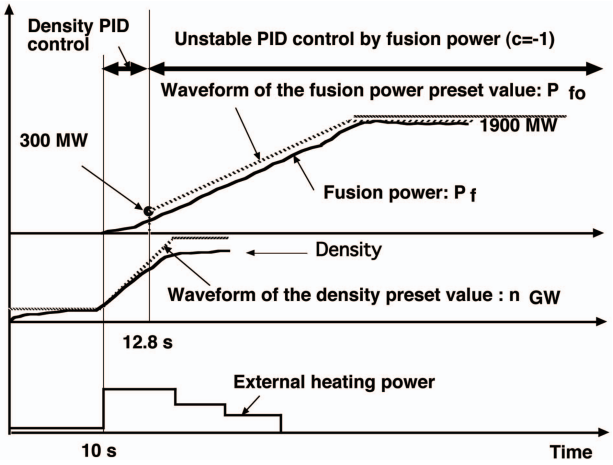

Fig. 4 The detailed schematic waveform on the transition phase from the density to fusion power control

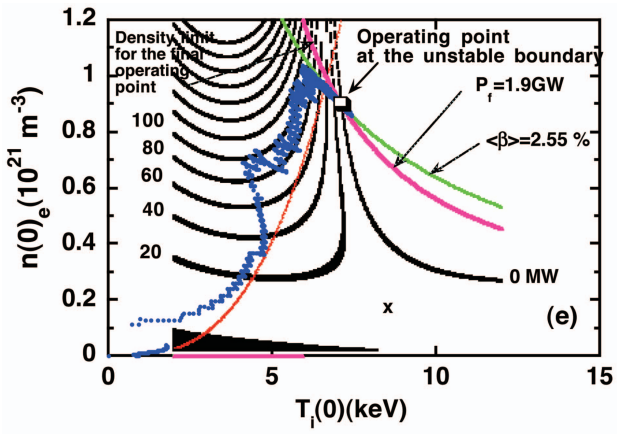

Fig. 5 The operation path (blue line) to the unstable ignition point on POPCON corresponding to Fig.3 (a).

nition. It was found in that paper [5] that lower alpha ash confinement time ratio provides lower plasma temperature, which is favorable for pellet penetration. Also the alpha ash confinement time ratio is simply estimated as $\tau_\alpha{}^*/\tau_E$ = 5.9 ~ 9 in LHD experiments using He gas puffing method, although further careful study is necessary. Therefore, in this study we have used the somewhat optimistic value of $\tau_\alpha{}^*/\tau_E$ = 5, and more optimistic values of 3 to expand the ignition regime for studying ignition characteristics to the various disturbances.

As the confinement time is increased to 4.1 s due to high-density operation, the plasma conduction loss P_L is decreased, reducing the divertor heat load to Γ_{div} ~6.3 MW/m^2 for the assumed 10 cm wetted width of the divertor plate at the right angle to the magnetic field line. The divertor heat load becomes a half when the divertor plate is inclined at 30 degree from the magnetic field line. However, as the heat load peaking factor is not taken into account in this simple estimation, further detailed analysis would be necessary. In this study we use 10 cm width of the divertor plate at the 90 degree angle to the magnetic field line as a reference for comparison.

The ratio of the bremsstrahlung loss power P_B to the alpha heating power P_α is as large as P_B/P_α ~70 %. The variation of the diverter heat flux is $\Delta\Gamma_{div}/\Gamma_{div}$ ~0.5/6.3 = 8 %, and variation of the first wall heat flux is $\Delta P_{HF}/P_{HF}$ ~ 0.018/0.23 = 8 %.

In Fig. 5 is shown the operation path to the unstable ignition point on POPCON corresponding to Fig. 3 (a). The operation is stabilized by cooling with fueling and by heating with the fueling reduction, which is controlled by the error of the fusion power $e_{DT}(P_f) = -(1 - P_f/P_{fo})$. We see that the operating point never go beyond 7.2 keV, which may avoid the neo-classical transport.

For the larger pellet size of 16 mm, ignition can be accessed although the density variation becomes as large as Δn ~8×10^{19} m^{-3}. For the larger pellet size of 17 mm, ignition is terminated at t = 50 s due to large density variation. At the termination phase, the density and the temperature are both decreased at the same time, and their variations are in phase. The plasma parameters during ignition access using 12 mm size pellet injection are of course more continuous, as already shown in Fig. 3 in the paper [5]. A smaller pellet size injection leads to the thermally unstable operation due to the shortage of fuel particles. In a future study, further optimization considering the pellet penetration and parameter variation would be necessary using the 1-D transport code.

5. PID Operation Parameters with Pellet Injection

So far, the integration time of T_{int} = 8 s and the derivative time of T_d = 0.26 s have been used for fueling control. By adjusting these time constants, the fusion power waveform can be optimized.

For example, in the case of T_{int} = 45 s and T_d = 0.39 s as shown in Fig. 6, the fusion power rise-up is delayed due to decrease in the temperature by frequent pellet injection just after 12.8 s which is caused by the large derivative term. Advancing the phase by the large derivative time rather delays the fusion power rise-up. This time delay can be improved by the feedback control of the heating power. However, as 100 MW heating power should be applied for a long time, it is not efficient at all.

On the other hand, the fusion power rise-up is not delayed by the smaller derivative time of T_d = 0.001 s as shown in Fig. 7. As the calculation time step is Δt = 0.02 s, corresponding to T_d ~0, the derivative term does not play any role. Therefore, just after 12.8 s, pellets are not injected due to negligible derivative term. Thus, the temperature does not decrease and the fusion power rises up linearly. Although the heating power helps the operation, fueling should be optimized at first by these control parameters.

The ignited operational regime with respect to the integration time T_{int} and derivative time T_d is shown in Fig. 8.

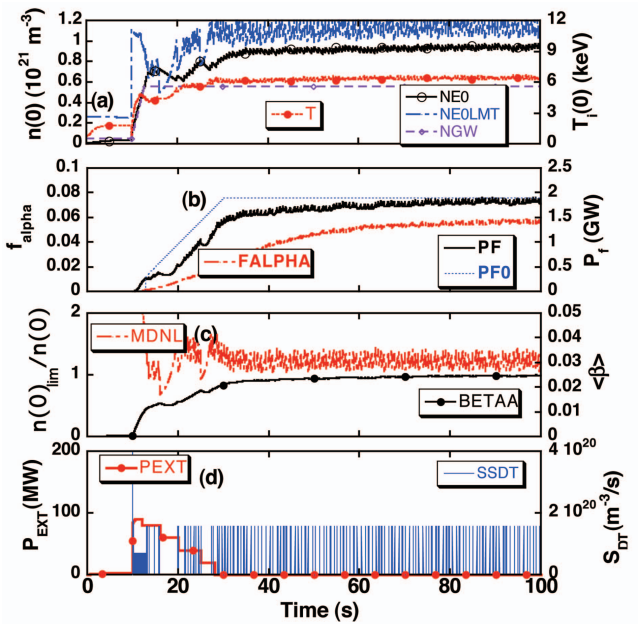

Fig. 6 Temporal evolution of the plasma parameters for $T_{\rm int}$ = 45 s and $T_{\rm d}$ = 0.39 s. The fusion power delays with respect to the set value for $\tau_\alpha{}^*/\tau_{\rm E}$ = 3.

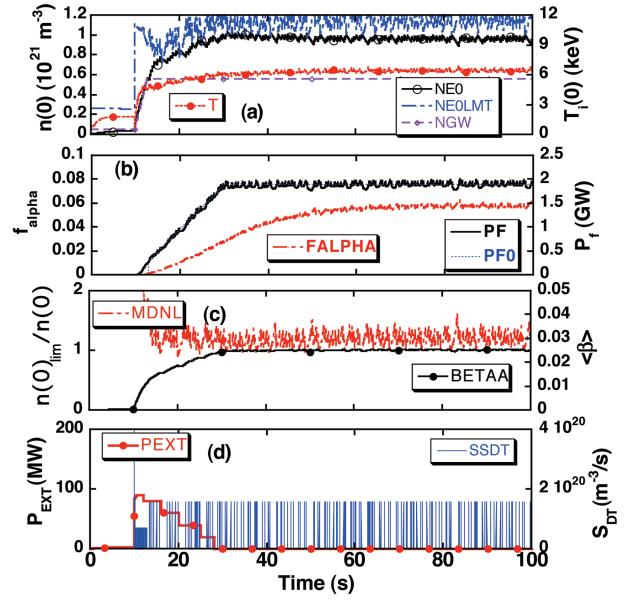

Fig. 7 Temporal evolution of the plasma parameters for $T_{\rm int}$ = 45 s and $T_{\rm d}$ = 0.001 s with the pellet size of 14 mm. The fusion power is not delayed with respect to the set value.

In this study $T_{\rm int}$ = 8 s and $T_{\rm d}$ = 0.26 s are used unless otherwise noted. It is seen that the operation regime is expanded by the feedback control of the heating power.

6. Control Robustness to the Disturbances with/without Heating Power Feedback Control

Without heating power feedback control, ignition can

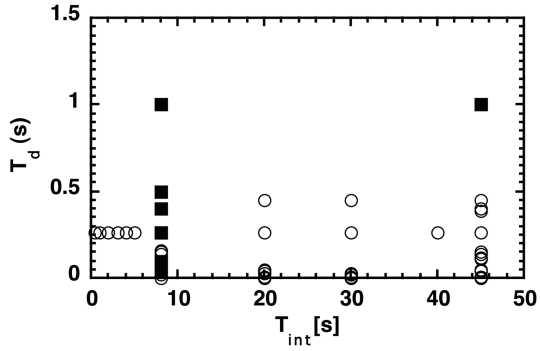

Fig. 8 Operation regime for the integration and derivative times for 14 mm pellet. Open circle shows without the heating power feedback and solid square with the heating power feedback.

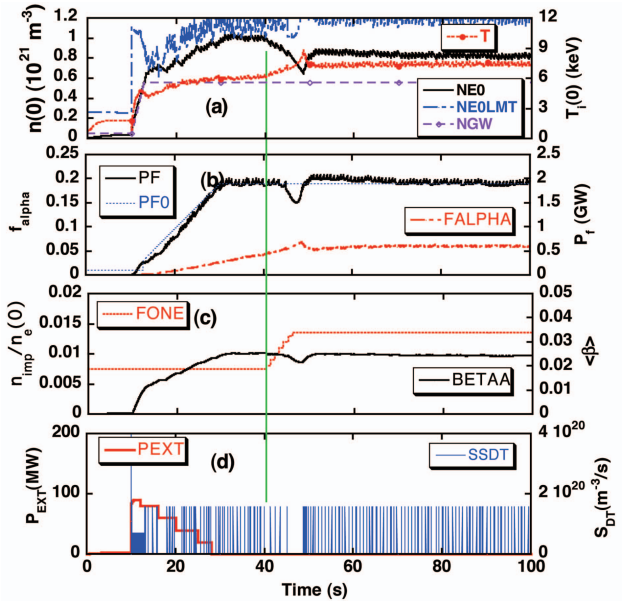

Fig. 9 Temporal evolution of the plasma parameters after impurity increment from $f_{\rm o}$ = 0.0075 to 0.013. Ignition is maintained by fueling control alone.

be maintained by the feedback control of the pellet fueling alone when the impurity fraction is increased from $f_{\rm o}$ = 0.0075 to 0.013 as shown in Fig. 9. When impurity fraction is larger than 0.013, ignition is terminated.

However, when the heating power feedback control is switched on at 15 s, the heating power is automatically applied and reduced to zero after some oscillation as shown in Fig. 10. When the impurity fraction is increased up to $f_{\rm o}$ = 0.021 after 40 s, the heating power is automatically applied to prevent the fusion power drop during impurity increment as shown in Fig. 10, and then ignition is recovered. Thus, feedback application of the heating power is found to be effective to keep ignition when disturbances exist.

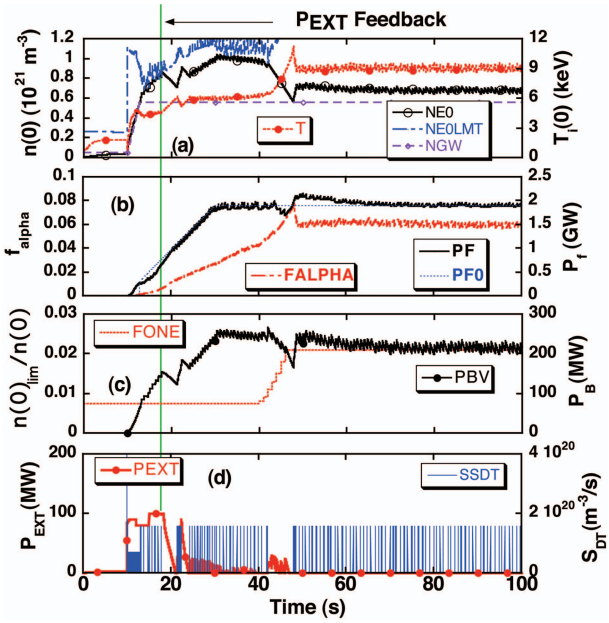

Fig. 10 Temporal evolution of the plasma parameters after impurity increment from $f_o = 0.0075$ to 0.021. Ignition is maintained by fueling and heating power feedback control.

7. Shutdown in the Unstable Operation

The fusion power shutdown is also important for ending discharge and machine operation. It was studied whether shutdown can be done without problems with the feedback control of pellet injection alone. In Fig. 11 is shown the shutdown phase using the preprogram of the heating power. In the late shutdown phase after 70 s, the external heating power of 20 MW is applied for smoother shutdown. The divertor heat load does not increase at all during the shutdown phase. For smooth fusion power shutdown the heating power should be applied because the operating point should pass the contour map of the heating power on POPCON to come back to the initial low temperature and density regime. Therefore, when the heating power is not applied during the fusion power shutdown phase, the fusion power abruptly decreases.

When the fueling is stopped at 65 s during the shutdown phase, the control of operation is lost, and the fusion power is excessive and the divertor heat load would increase to 39 MW/m^2 for the 10 cm divertor plate with the right angle to the magnetic field line as shown in Fig. 12. Therefore in the shutdown phase, fueling should not be stopped when operated in the unstable ignition regime. A large quantity of fueling provides rather safer operation in the whole discharge.

When feedback control of the external heating power is applied at 15 s during the fusion power rise up phase, the heating power is automatically switched off and then automatically applied during the shutdown phase. But as calculation was terminated before 80 s, after 75 s in the late

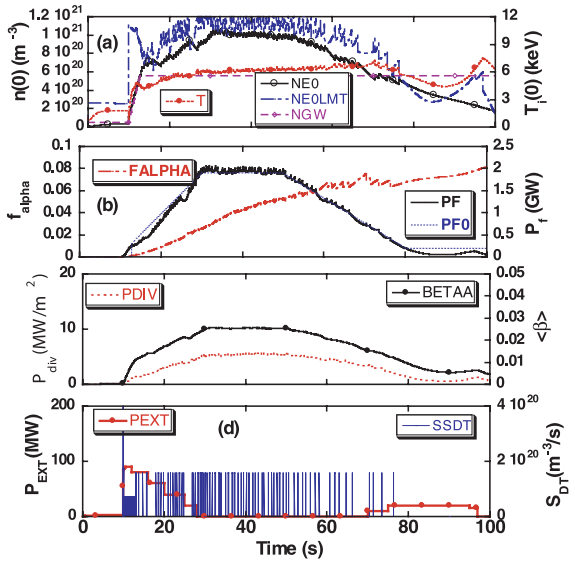

Fig. 11 Temporal evolution of the plasma parameters during the shutdown phase without the heating power feedback control.

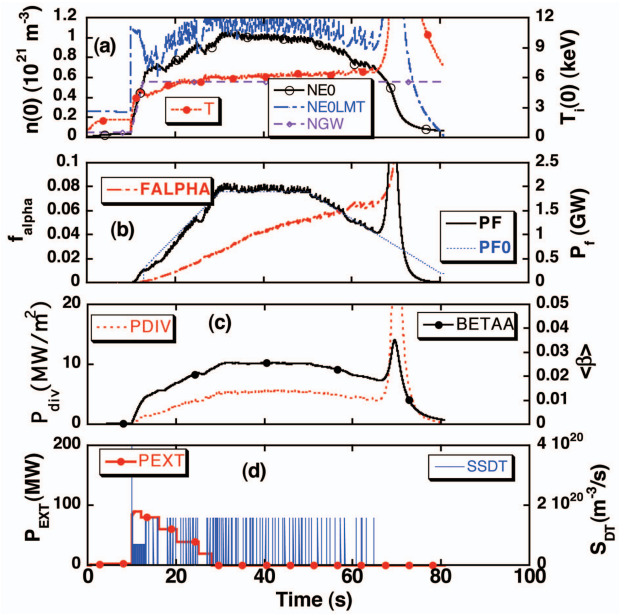

Fig. 12 Temporal evolution of the plasma parameters during the shutdown phase without the heating power feedback control. At 65 s fueling is stopped externally.

shutdown phase the heating power of 20 MW was applied for smoother shutdown.

8. Discussion and Summary

In this study we have used a confinement factor of 1.6, and the helium ash confinement time ratio of τ_α^*/τ_E = 3 and 5. Detailed studies were conducted for other parameters [5]. To lower the operating temperature for good pellet penetration, the helium ash confinement time ratio should be as small as possible.

In this study we demonstrated that thermally unstable ignited operation is stabilized when the pellets are injected repetitively. The operational regime is expanded when the feedback control of the heating power based on the fusion power is applied as well as fueling.

Unstable ignition control used in this study is robust to disturbances such impurity injection during the discharge with the feedback control of the heating power. However, as we studied the transient response to the preset value and disturbances only in an ignited operation, further studies are required for the unified control algorithm applicable to ignition and sub-ignition.

However, it is still a big issue which heating system is employed in the high density operation. As a neutral beam heating needs a very high energy (for example ~5 MeV for the penetration length of 0.7 m at $n(0) \sim 1 \times 10^{21}\,\mathrm{m}^{-3}$), it can be used alone in a very early lower-density phase. An electron Bernstein wave (EBW) heating may be a candidate for a heating system [18]. Therefore, active study on EBW heating in a high density regime is required. The heating power was continuously applied to study overall response behavior in a feedback control phase in this study. As the heating power would be applied in a step like manner in an actual situation, it may slightly alter the time response.

This work is performed with the support and under the auspices of the National Institute for Fusion Science (NIFS) Collaborative Research Program NIFS04KFDF001, NIFS05ULAA116 and NIFS07KFDH002.

[1] N. Ohyabu, T. Morisaki, S. Masuzaki *et al.*, Phy. Rev. Lett. **97**, 055002-1 (2006).
[2] R. Sakamoto *et al.*, in 21th IAEA conference (Geneva, Switzerland, Oct 13, 2008) EX/8-1Ra.
[3] O. Mitarai, A. Sagara, N. Ohyabu, R. Sakamoto, A. Komori and O. Motojima, Plasma Fusion Res. **2**, 021 (2007).
[4] O. Mitarai, A. Sagara, N. Ohyabu, R. Sakamoto, A. Komori and O. Motojima, Fusion Sci. Technol. **56**, 1495 (2009).
[5] O. Mitarai, A. Sagara, N. Ashikawa, R. Sakamoto, M. Yoshinuma, M. Goto, T. Morisaki *et al.*, in 21th IAEA conference (Geneva, Switzerland, Oct 13, FT/P3-19 2008).
[6] K. Maki, Fusion Technol. **10**, 70 (1986).
[7] J. Mandrekas and W.M. Stacy Jr., Fusion Technol. **19**, 57 (1991).
[8] E. Bebhan and U. Vieth, Nucl. Fusion **37**, 251 (1996).
[9] W. Hui *et al.*, Fusion Technol. **25**, 318 (1994).
[10] E. Schuster *et al.*, Fusion Sci. Technol. **43**, 18 (2003).
[11] J.E. Vitela and J.J. Martinell, Plasma Phys. Control. Fusion **40**, 295 (1998).
[12] U. Stroh, M. Murakami, R.A. Dory, H. Yamada, S. Okamura, F. Sano and T. Obiki, Nucl. Fusion **36**, 1063 (1996).
[13] S. Sudo, Y. Takeiri, H. Zushi, F. Sano, K. Itoh, K. Kondo and A. Iiyoshi, Nucl. Fusion **30**, 11 (1990).
[14] P.C. Souers, *Hydrogen Properties for Fusion Energy* (University of California Press, 1986) p.80.
[15] O. Mitarai, A. Oda, A. Sagara, *et al.*, Fusion Eng. Des. **70**, 247 (2004).
[16] O. Mitarai, A. Sagara *et al.*, Nucl. Fusion **47**, 1411 (2007).
[17] O. Mitarai and K. Muraoka, Nucl. Fusion **39**, 725 (1999).
[18] H.P. Laqua, V. Erckmann *et al.*, Phys. Rev. Lett. **78**, 3467 (1997).